IAC-13-C2.5.4

SHAPE-CHANGING SOLAR SAILS FOR NOVEL MISSION APPLICATIONS

Andreas Borggräfe
Advanced Space Concepts Laboratory, Department of Mechanical and Aerospace Engineering,
University of Strathclyde, Glasgow, Scotland G1 1XJ, United Kingdom,
E-Mail: andreas.borggraefe@strath.ac.uk

Jeannette Heiligers
Advanced Space Concepts Laboratory, Department of Mechanical and Aerospace Engineering,
University of Strathclyde, Glasgow, Scotland G1 1XJ, United Kingdom,
E-Mail: jeannette.heiligers@strath.ac.uk

Matteo Ceriotti
School of Engineering, University of Glasgow, Glasgow, Scotland G12 8QQ, United Kingdom,
E-Mail: matteo.ceriotti@glasgow.ac.uk

Colin R. McInnes
Advanced Space Concepts Laboratory, Department of Mechanical and Aerospace Engineering,
University of Strathclyde, Glasgow, Scotland G1 1XJ, United Kingdom,
E-Mail: colin.mcinnes@strath.ac.uk

In order to increase the range of potential mission applications of solar sail technology, this paper introduces the concepts of shape change and continuously variable optical properties to large gossamer spacecraft. Merging the two concepts leads to the idea of solar sails as multi-functional platforms that can have potential benefits over conventional solar sails by delivering additional key mission functions such as power collection, sensing and communications. To this aim, the paper investigates the static deflection of a thin inelastic circular sail film with a variable surface reflectivity distribution. The sail film is modelled as a single surface framed by a rigid supporting hoop structure. When changing the reflectivity coefficient across the sail surface, the forces acting on the sail can be controlled without changing the incidence angle relative to the Sun. In addition, by assigning an appropriate reflectivity function across the sail, the load distribution due to solar radiation pressure can also be manipulated to control the billowing of the film. By an appropriate choice of reflectivity across the sail, specific geometries can be generated, such as a parabolic reflector, thus enabling a multi-functional sail. This novel concept of optical reconfiguration can potentially extend solar sail mission applications.

I. INTRODUCTION

Using conventional solar sailing technology, the solar radiation pressure (SRP) force vector direction and magnitude depend strongly on the sail attitude relative to the Sun, limiting the applicability of solar sails compared to other low-thrust propulsion systems such as solar-electric propulsion. Furthermore, the SRP force magnitude follows an inverse square law with solar distance, making the sail less efficient at large distances from the Sun.[1] In order to increase the flexibility of modulating the SRP force and to increase the range of potential solar sail mission applications, we introduce the concepts of shape change and variable optical properties for large gossamer spacecraft.[2] Merging these concepts, potential benefits of such a system over conventional solar sails can be identified. It is envisaged to use future shape-changing solar sails as multi-functional platforms that can deliver additional key mission functionality such as power collection, sensing and communications. For example, the sail may begin at Earth escape in a flat configuration on a small-body science mission towards a designated target object. In close proximity to the target body, the sail reconfigures to a parabolic shape, using its reflective film as a remote sensing device or as a large communication antenna, before continuing again in a flat thrust mode.

To demonstrate these capabilities of solar sails, this paper investigates the use of variable film reflectivity for shape deflection control of a circular sail. When changing the reflectivity coefficient across the sail film, the SRP forces acting on a segment of the sail can be controlled without changing the incidence angle relative to the Sun and without using additional attitude control actuators. The reflectivity can be modified using electrochromic coatings, which consist of an electro-active material that changes its surface reflectivity according to an applied electric potential.[3] As an alternative, the thin sail film could also be pre-fabricated with a fixed surface reflectivity distribution that allows for a parabolic deflection, since it will be shown in this paper that the nominal sail deflection due to SRP is not ideal paraboloid. Either way, by assigning an appropriate reflectivity function across the sail area, the local SRP load distribution acting on the thin sail film can be controlled, manipulating its nominal deflection shape.

In doing so, the solar sail is modelled as a thin inelastic circular film, attached to a rigid supporting hoop structure, as shown in Fig. 1. The mass of the hoop is assumed to be much larger than the sail film. The film is not spanned tightly but suspended in a slack manner to yield controlled inelastic billowing.

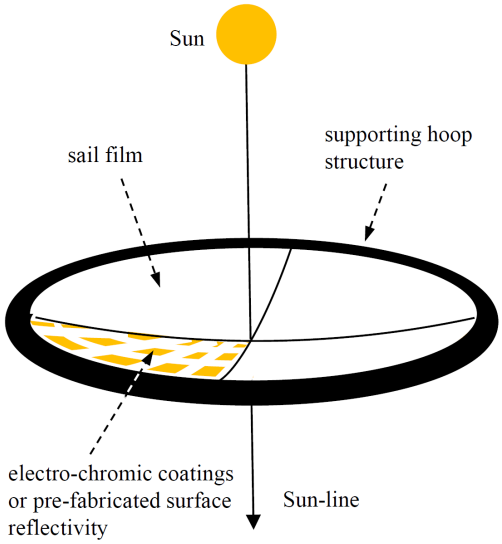

Figure 1: Circular sail film attached to rigid hoop structure, with electro-chromic coatings and/or pre-fabricated surface reflectivity

The governing equations of inelastic deflection of thin surfaces subject to a distributed SRP loads are presented in section II, derived from idealising the 2-dimensional (2-D) sail surface as a 'cobweb' of radially spanned threads that are not linked in the circumferential direction. The threads are suspended from the rigid hoop

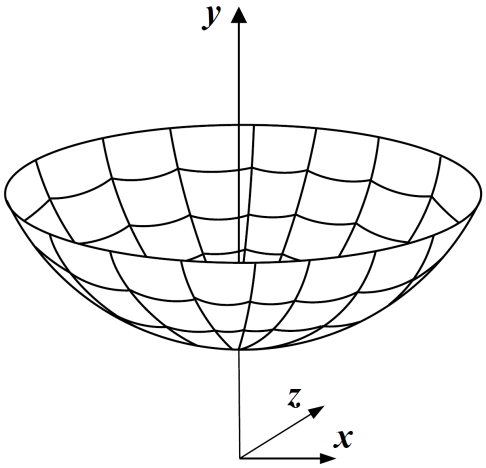

Figure 2: Circular sail film modelled as an inelastic 'cobweb' of radially spanned threads, suspended by a rigid supporting hoop structure. The circumferential threads are carrying no tension and are not considered in the model

structure and intersect at the centre of the circular film, as can be seen in Fig. 2. This way, the surface can be approximated as a set of 1-dimensional (1-D) catenary-type curves that can be investigated semi-analytically rather than through finite-element analysis. Circumferential tension in the slack inelastic film is assumed to be zero, thus having no impact on the validity of the concept. In general, catenary curves are found widely in suspension bridges and cables. They are used in architecture and engineering, for example in the design of bridges and arches, because the absorbed forces do not result in bending moments.[4] In section III, the resulting deflection curves of different inelastic sail films due to a uniform vertical SRP load are presented. The circular films have a varying slack diameter, suspended from a rigid hoop structure of a fixed $200\,\mathrm{m}$ diameter. By increasing the total length of the film, thus by suspending more material in between the fixed hoop, the sag of the reflective film can be controlled. Through this, the focal length of the deflected surface can be changed, enabling a range of new applications of solar sails. Since the deflected film shapes are not ideal paraboloids, as necessary to be used as an antenna or solar concentrator, section IV discusses manipulation of the nominal deflection curves through the use of suitable reflectivity functions across the surface. It is shown that when a particular deflection shape is selected a priori (e.g. a parabolic shape to form an antenna), the required reflectivity distribution can be calculated by formulating an inverse problem. Finally, resulting paraboloid-type deflection shapes and deflection magnitudes are assessed in terms of their focal length and thus their usefulness for novel mission applications.

II. EQUATIONS OF INELASTIC SAIL FILM DEFLECTION

The problem of inelastic deflection of a thin circular sail film of uniform thickness, subject to uniform vertical SRP load distribution, is addressed first. Later, in section IV, the same configuration under non-uniform load due to distributed reflectivity is analysed. The circular film is modelled as a 1-dimensional slack inelastic catenary-like chain, as shown in Fig. 3. Through this simplification, only radial forces in the circular inelastic film are considered, while circumferential forces are zero. The sail film is supported by a rigid circumferential hoop structure, forming hinged-support type boundary conditions at the edges. The mass of the hoop is assumed to be much larger than the sail film. The basic equations of a classical inelastic catenary curve in uniform gravity are described first, followed by the extension of the model introducing a uniform SRP load distribution.

II.I EQUATIONS OF A HANGING CHAIN

The governing equation of the classical inelastic flexible 1-D catenary deflection due to gravity, as shown in Fig. 3, can be found in the literature.[5] It was first derived by Leibniz, Huygens and Bernoulli in 1691.[6] The

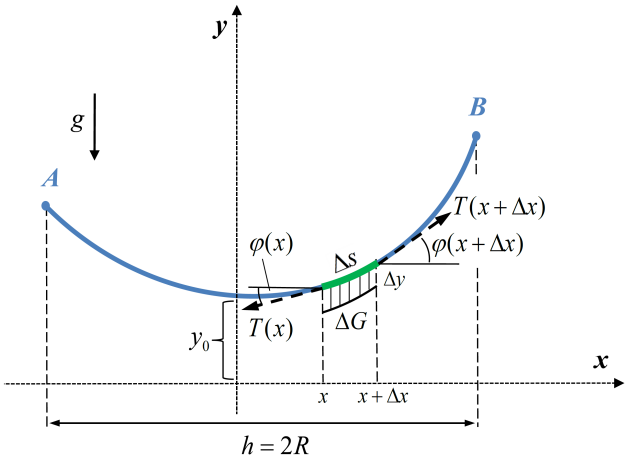

Figure 3: Force equilibrium over segment Δs of classical catenary curve in vertical uniform gravitational field

mathematical model idealises the chain by assuming that it is thin enough to be regarded as a 1-dimensional curve. Here, inelastic means the chain material is infinitely rigid to axial forces (i.e. in the tangential direction). Fully flexible means the infinitesimal chain links are connected by friction-free hinges and thus cannot absorb bending moments. Consequently, any tension force exerted on the chain is parallel to the chain. The differential equation describing the static inelastic deflection (as a function of the position x along the curve) is derived from the equilibrium of forces over a curve segment. Considering a small chain element of length Δs, according to Fig. 3, the forces are the distributed gravity force

$$\Delta G = \tau g A \, \Delta s \tag{1}$$

where τ is the density of the chain material, g is the gravitational acceleration and A is the cross-sectional area of the element, and further, the tension forces $T(x)$ and $T(x+\Delta x)$, respectively, at points x and $(x+\Delta x)$. The angle φ denotes the local pitch angle of the element between the **x**-axis and the tangential direction. The equilibrium conditions of an element of length Δs in the **x** and **y** (vertex) direction can be written as

$$-T(x)\cos\varphi(x) + T(x+\Delta x)\cos\varphi(x+\Delta x) = 0 \tag{2a}$$

$$-T(x)\sin\varphi(x) + T(x+\Delta x)\sin\varphi(x+\Delta x) = \Delta G \tag{2b}$$

It can be seen from Eq. 2a that the horizontal tension component is always constant along x. The resulting ordinary differential equation (ODE) describing the deflected catenary can be obtained using analytical methods[5]

$$y'' = \frac{\tau g A}{T_0}(1+y'^2)^{1/2} \tag{3}$$

with the tension at the centre T_0. The catenary coefficient $a_{\mathrm{cat}} = T_0/(\tau g A)$ determines the geometrical shape of the catenary curve, as will be described below.

The solution of the deflection curve of the catenary can be obtained analytically as

$$y_{\mathrm{cat}}(x) = a_{\mathrm{cat}} \cosh\left(\frac{x}{a_{\mathrm{cat}}}\right) + c_{\mathrm{cat}} \tag{4}$$

with coefficients $a_{\mathrm{cat}} = T_0/(\tau g A)$ and c_{cat}, both in units of $[\mathrm{m}]$. The two coefficients together define the deflection $y_{0,\mathrm{cat}}$ at the centre, where $\cosh(0) = 1$. Assuming the two suspension points are on the **x**-axis, with the distance of the two suspension points being the span $h = 2R$, the coefficient c_{cat} can now be calculated using $y_{\mathrm{cat}}(R) = 0$, such that

$$c_{\mathrm{cat}} = -a_{\mathrm{cat}} \cosh\left(\frac{R}{a_{\mathrm{cat}}}\right) \tag{5}$$

and hence the central deflection is

$$\begin{aligned} y_{0,\mathrm{cat}} &= a_{\mathrm{cat}}\cosh(0) + c_{\mathrm{cat}} \\ &= a_{\mathrm{cat}}\left(1 - \cosh\left(\frac{R}{a_{\mathrm{cat}}}\right)\right) \end{aligned} \tag{6a}$$

The resulting catenary curve when setting $a_{\mathrm{cat}} = 1$ and $R = 1$ is shown in Fig. 4, together with a parabolic reference curve of the same sag y_0. As can be seen in

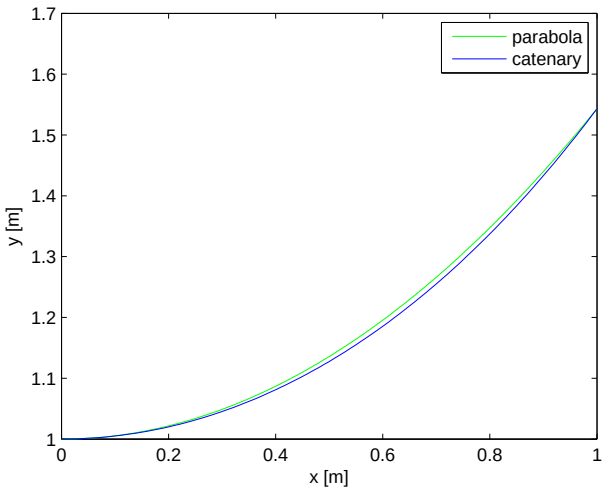

Figure 4: Comparison of catenary curve $y_{\mathrm{cat}}(x) = \cosh(x)$ and parabolic curve $y_{\mathrm{p}}(x) = (\cosh(1) - 1)x^2 + 1$ of same sag and span

Fig. 4, the two curves are slightly different, with the catenary curve being more extended towards the edge, thus showing a higher deflection than the parabola. As a note of history, it was only in 1669 when Jungius disproved Galileo's claim that the curve of a chain hanging under gravity would be a parabola.[5]

According to Eq. 4, the coefficient a_{cat} completely defines the shape of the catenary curve. How a_{cat} can be calculated will be shown in the following. Fig. 5 shows the catenary shape for decreasing values of $a_{\mathrm{cat}} = T_0/2p_0$, thus decreasing ratios of tension to load.

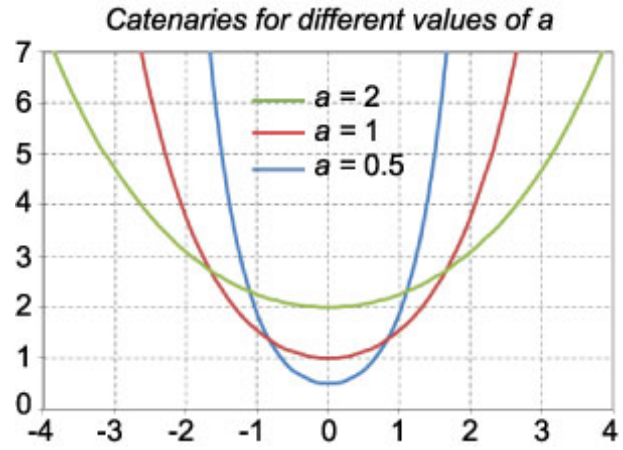

Figure 5: Comparison of catenary curves for decreasing values of $a_{\mathrm{cat}} = T_0/2p_0$ (ratio of tension to load)

It becomes clear that with smaller central tension T_0, the sagging increases. In other words, the higher the sag of the 'hanging' chain, the smaller the central tension between the two catenary arms connected at the centre. Further, even without knowing the central tension force T_0 directly, a_{cat} can be calculated when introducing the additional constraint for the total curve length. Without derivation, the total arc length S_{cat} of the catenary curve can be calculated as

$$S_{\mathrm{cat}} = 2\,a_{\mathrm{cat}} \sinh\left(\frac{h}{2a_{\mathrm{cat}}}\right) \tag{7}$$

This transcendental equation in a_{cat} can only be solved numerically. Inserting the a_{cat} obtained for a specific nominal catenary length S_{cat} and span h into Eq. 4 results in the corresponding deflection curve. Thus, knowing the value of T_0 is not necessary to find the coefficient a_{cat}, because it is only a function of h and S_{cat}. Moreover, changing the load magnitude p_0 does not affect the shape of the catenary curve. This result is plausible, since increasing the load on a deflected inelastic chain cannot deflect the chain further (unless it breaks). Instead, it increases the in-curve tension T_0 accordingly, to keep the coefficient a_{cat}, and thus the ratio of tension to load, constant.

II.II EXTENDED EQUATIONS USING SOLAR RADIATION PRESSURE

The previously described deflection model of an inelastic catenary is now extended by introducing a uniform vertical SRP load, as shown in Fig. 6. The SRP

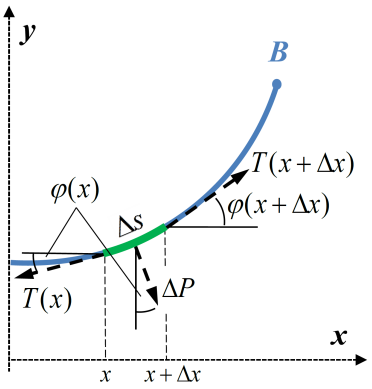

Figure 6: Force equilibrium over segment Δs of catenary curve under uniform vertical SRP load

force acting on the sail film is calculated using a simplified SRP model.[1] It assumes that the sail surface is a perfectly (specular) reflecting mirror, neglecting all other forms of optical interactions between the solar photons and the sail surface such as diffuse reflection, absorption and thermal re-emission. Therefore, the SRP exerted on

a surface of reflectivity ρ is

$$P = p_0(1+\rho)\Big(\frac{R_{\mathrm{S},0}}{R_\mathrm{S}}\Big)^2 \cos^2\varphi \tag{8}$$

at a radial distance R_S from the Sun, with the pitch angle φ between the Sun-sail line and the sail plane normal and (again) $p_0 = 4.563\times10^{-6}\ \mathrm{N/m^2}$ the solar radiation pressure at $R_{\mathrm{S},0} = 1\,\mathrm{AU}$. In the following, the undeflected sail surface is assumed to be always perpendicular to the Sun, thus $\varphi = 0$, at a solar distance of 1 AU. At first, a constant reflectivity $\rho = 1$ is chosen, which reduces the SRP load on the sail film to $P = 2p_0$.

The differential equation system describing the static deflection is derived from the equilibrium of forces along the sail film curve (see Fig. 6). Considering again the force equilibrium of a small chain element of length Δs, the forces acting on a section of the chain are now the distributed SRP force (per unit length)

$$\Delta P = 2p_0\Delta s \tag{9}$$

and the tension forces $T(x)$ and $T(x+\Delta x)$, respectively, at points x and $(x+\Delta x)$. The equilibrium conditions of an element of length Δs in **x** and **y** direction are written as

$$\begin{aligned} -T(x)\cos\varphi(x) + T(x+\Delta x)\cos\varphi(x+\Delta x) &= -2p_0\sin\varphi(x)\Delta s \end{aligned} \tag{10a}$$

$$\begin{aligned} -T(x)\sin\varphi(x) + T(x+\Delta x)\sin\varphi(x+\Delta x) &= \quad 2p_0\cos\varphi(x)\Delta s \end{aligned} \tag{10b}$$

It can be seen that, in contrast to the deflection of a hanging chain in a gravitational field, SRP causes a horizontal force component in x-direction, depending on the local pitch angle with the surface normal. Dividing both equations by Δx and taking the limit $\Delta s \to 0$, while introducing the arc length equation

$$\Delta s = \sqrt{\Delta x^2 + \Delta y^2} \tag{11}$$

for an arbitrary continuous curve segment in the **x**-**y** plane gives

$$\frac{\mathrm{d}}{\mathrm{d}x}\big(T\cos\varphi\big) = -2p_0\sin\varphi\sqrt{1+\Big(\frac{\mathrm{d}y}{\mathrm{d}x}\Big)^2} \tag{12a}$$

$$\frac{\mathrm{d}}{\mathrm{d}x}\big(T\sin\varphi\big) = \quad 2p_0\cos\varphi\sqrt{1+\Big(\frac{\mathrm{d}y}{\mathrm{d}x}\Big)^2} \tag{12b}$$

Using elementary trigonometric relations, the $\sin\varphi$ and $\cos\varphi$ expressions can be written as

$$\sin\varphi = \frac{\mathrm{d}y}{\mathrm{d}x}\Big(1+\Big(\frac{\mathrm{d}y}{\mathrm{d}x}\Big)^2\Big)^{-1/2} \tag{13a}$$

$$\cos\varphi = \quad \Big(1+\Big(\frac{\mathrm{d}y}{\mathrm{d}x}\Big)^2\Big)^{-1/2} \tag{13b}$$

Inserting into Eq. 12 and rewriting results in

$$\frac{\mathrm{d}T}{\mathrm{d}x}\Big(1+\Big(\frac{\mathrm{d}y}{\mathrm{d}x}\Big)^2\Big)^{-\frac{1}{2}} = -2p_0\frac{\mathrm{d}y}{\mathrm{d}x} \tag{14a}$$

$$\Big(\frac{\mathrm{d}T}{\mathrm{d}x}\frac{\mathrm{d}y}{\mathrm{d}x} + T\frac{\mathrm{d}^2y}{\mathrm{d}x^2}\Big)\Big(1+\Big(\frac{\mathrm{d}y}{\mathrm{d}x}\Big)^2\Big)^{-\frac{1}{2}} = 2p_0 \tag{14b}$$

which can be reformulated as two coupled ODEs in terms of the vertical deflection $y(x)$ along x and the in-curve tension $T(x)$ as

$$T' = -2p_0y'(1+y'^2)^{1/2} \tag{15a}$$

$$y'' = \frac{2p_0}{T}(1+y'^2)^{1/2} - \frac{T'}{T}y' \tag{15b}$$

Inserting Eq. 15a in 15b returns the static ODE system of flexible, inelastic deflection of a slack catenary-like sail film due to vertical SRP load distribution

$$T' = -2p_0y'(1+y'^2)^{1/2} \tag{16a}$$

$$y'' = \frac{2p_0}{T}(1+y'^2)^{3/2} \tag{16b}$$

It is useful to reformulate the system further in order to eliminate $T(x)$. When substituting $z = y'$ and dividing such as

$$\frac{\mathrm{d}T}{\mathrm{d}z} = \frac{\mathrm{d}T/\mathrm{d}x}{\mathrm{d}z/\mathrm{d}x} = -zT(1+z^2)^{-1} \tag{17}$$

and separating variables, Eq. 17 can be integrated to obtain an expression for $T(x)$

$$T(x) = \frac{D}{\sqrt{1+z^2}} = \frac{T_0}{\sqrt{1+y'^2}} \tag{18}$$

with D an integration constant. For any symmetric load distribution across the circular sail, the slope of deflection is always zero at the centre, thus $y'(0) = 0$. Inserting this condition into Eq. 18, it can be seen that the integration constant D represents the tension force T_0 at the centre. Inserting the expression into Eq. 16b, the system simplifies into a single equation

$$y'' = \frac{2p_0}{T_0}(1+y'^2)^2 \tag{19}$$

This 2nd order ODE has no explicit solution, however, an implicit solution can be found as

$$\frac{y'}{1+y'^2} + \arctan(y') = \frac{2p_0}{T_0}x + C_1 \tag{20}$$

with $C_1 = 0$ when using again the condition $y'(0) = 0$. The simplified ODE (Eq. 19) can be solved as a boundary value problem (BVP) on the interval $I = [a, b]$, with $a = 0$ at the centre of the circular sail film and $b = R$ at the edge. While for the classical catenary under uniform gravitational load the central tension T_0 does not need to be known to obtain the deflection curve, for solving Eq. 19, the actual value for T_0 must be specified. Due to this, the 2nd order BVP needs a third boundary condition (BC) to be solved numerically, e.g. using the MATLAB™ *bvp4c* routine that employs a three-stage Lobatto IIIa collocation method.[7] Assuming hinged support at the edge, the BCs are

$$y(R) = 0, \qquad y'(0) = 0, \qquad T(0) = T_0 \tag{21}$$

In order to find T_0, a twofold approach is applied in the following. First, an initial guess $T_{0,\text{init}}$ is generated from Eq. 16b, assuming $T(x)$ to be constant along x. The corresponding deflection curve is denoted by y_{init} and y'_{init}. Second, through iteration of the BVP using increments $T_{0,i+1} = T_{0,i} + \Delta T_0$, the correct T_0 is approximated using the additional constraint that the final deflection curve must satisfy a defined slack catenary length in terms of its total arc length

$$S = \int_0^R \sqrt{1+y'^2}\,\mathrm{d}x \stackrel{!}{=} S_{\text{nom}} \tag{22}$$

When fixing the deflection curve to a predefined value S_{nom}, each intermediate iteration returns the current $y'_i(x)$, using $T_{0,i}$, and calculates the total curve length $S_{i,\text{BVP}}$. The iteration finishes after a predefined threshold for the catenary length $|S_{\text{nom}} - S_{i,\text{BVP}}| \leq \lambda$ is satisfied, e.g. $\lambda = 1\text{mm}$.Note that the initial guess, assuming $T(x) = T_{0,\text{init}} = \text{const}$, can be generated from Eq. 16b through analytic integration, using the above BCs. This returns

$$y' = x\left[a_{\text{SRP}}^2 - x^2\right]^{-\frac{1}{2}} \tag{23a}$$

and so

$$y = -\left[a_{\text{SRP}}^2 - x^2\right]^{\frac{1}{2}} + \left[a_{\text{SRP}}^2 - R^2\right]^{\frac{1}{2}} \tag{23b}$$

with $a_{\text{SRP}} = T_{0,\text{init}}/2p_0$. Inserting Eq. 23a into the arc length equation (Eq. 22) gives

$$S(x) = a_{\text{SRP}} \cdot \tan^{-1}\left[\frac{x}{\left(a_{\text{SRP}}^2 - x^2\right)^{1/2}}\right] \tag{24}$$

and thus the deflected curve length as function of x and a_{SRP}. When a value for $S(R) = S_{\text{nom}}$ at the endpoint R of the curve is assigned, this transcendental function can be solved numerically for a_{SRP}. Inserting into the relation

$$T_{0,\text{init}} = a_{\text{SRP}} p_0 \tag{25}$$

completes the initial guess for solving the first iteration of the BVP.

III. RESULTS

The resulting inelastic sail film deflection due to uniform vertical SRP load distribution is shown in Fig. 7 for a rigid hoop of $h = 2R = 200\,\text{m}$ diameter (span) and slack length of the sail film of $S_{\text{nom}} = 105\,\text{m}$ radius. The result was obtained by solving the BVP with a threshold $\lambda = 1\text{mm}$. A rough linear estimate of the central deflection y_0 to be expected results from Pythagoras equation, $y_{0,\text{Pyth}} = \sqrt{S_{\text{nom}}^2 - R^2} = 32\,\text{m}$. Assuming that the deflected film surface is an approximated paraboloid, the corresponding focal length (see also section IV) can be obtained from

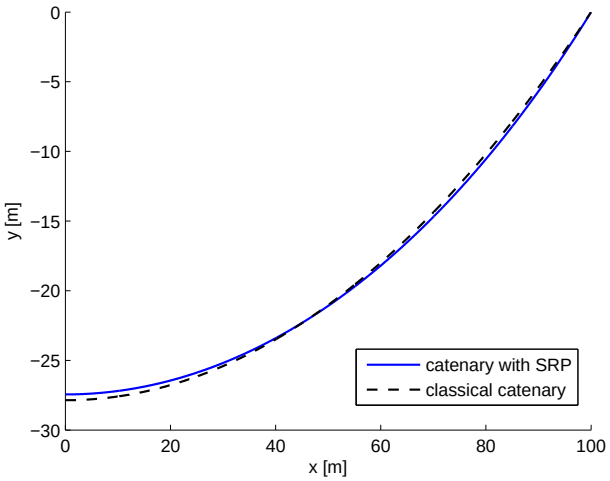

Figure 7: Comparison of catenary curve with SRP $S = 105\,\text{m}$ and classic catenary in gravitational field

$$f = \frac{1}{4a_{\text{p}}} = \frac{R^2}{2|y_0|} \tag{26}$$

with a_p the quadratic coefficient of the equivalent 2^nd order (parabolic) polynomial. For the example above, the focal length would be $78\,\mathrm{m}$. By positioning a detached platform at this distance from the sail surface, it could be used as an antenna or solar concentrator.

As can be seen from Fig. 7, the solution considering SRP is more displaced towards the edge and shows a smaller central deflection. This is due to the horizontal component of the distributed load as a function of the local pitch angle. The final value for the tension at the centre is $T_{0,\mathrm{init}} = 0.00183\,\mathrm{N/m}$, while the initial guess was $T_{0,\mathrm{final}} = 0.00178\,\mathrm{N/m}$, according to Eq. 25. The tension along the x axis is shown in Fig. 8. Throughout the following analysis, a supporting

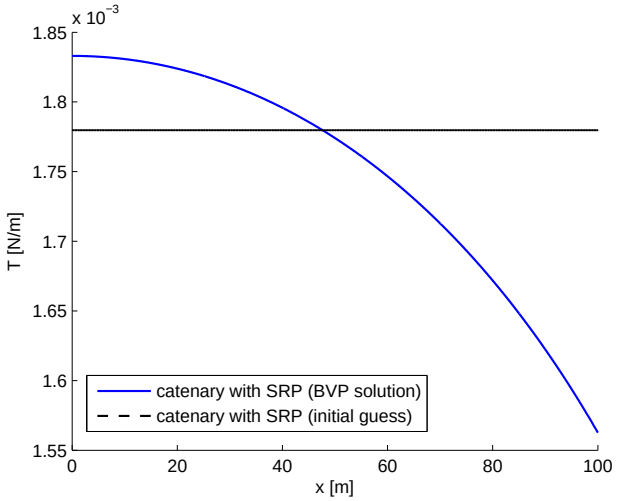

Figure 8: Resulting in-curve tension along catenary with SRP, as obtained from iterative solution of the BVP, and constant initial guess from analytic solution

rigid hoop structure of $200\,\mathrm{m}$ diameter will be used in all figures. The inelastic deflection curves with increasing nominal slack film length, are shown in Fig. 9 for $S_\mathrm{nom} = [101, 102, 103, 104, 105, 106]\,\mathrm{m}$.

IV. SAIL SHAPE CONTROL USING VARIABLE REFLECTIVITY DISTRIBUTION

In the following, the sail deflection shape is now controlled by varying the reflectivity across the sail surface to achieve parabolic shapes useful for using a reflective sail surface as an antenna, telescope or power collector.

In order to compare the resulting sail deflection curves with the ideal parabolic defection shape, the reference parabola needs to be defined first. Its curve must be of equal total arc length, since it results from the same sail film suspended by a rigid hoop of the same span. Assum-

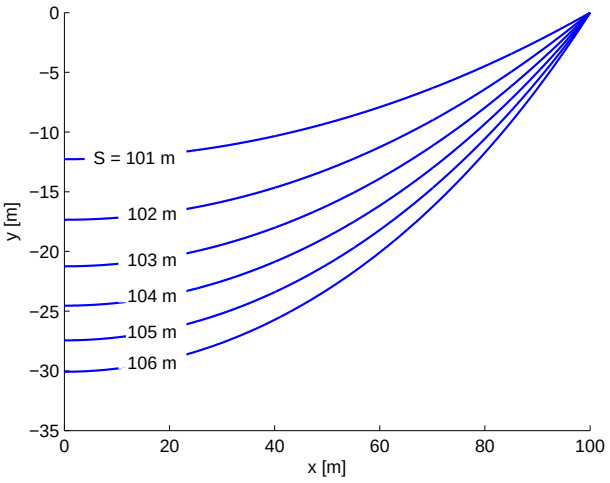

Figure 9: Inelastic sail film deflection due to uniform vertical SRP load for different nominal sail film lengths S_nom

ing a general parabolic deflection curve

$$y_\mathrm{p} = a_\mathrm{p}x^2 + b_\mathrm{p}x + c_\mathrm{p} \tag{27a}$$

$$y'_\mathrm{p} = 2a_\mathrm{p}x + b_\mathrm{p} \tag{27b}$$

$$y''_\mathrm{p} = 2a_\mathrm{p} \tag{27c}$$

and considering a symmetric load distribution, thus $y'(0) = 0$, the coefficient b_p is zero. The constant coefficient c_p represents the deflection value at the centre, thus

$$c_\mathrm{p} = y_0 \tag{28}$$

Inserting Eq. 27b into the arc length Eq. 22 yields

$$S_\mathrm{p} = \int_0^R \sqrt{1 + (2a_\mathrm{p}x)^2}\,\mathrm{d}x = \tag{29a}$$

$$\frac{1}{2}x\sqrt{1 + 4a_\mathrm{p}^2x^2} + \frac{1}{4a_\mathrm{p}}\mathrm{arsinh}(2a_\mathrm{p}x) + C_\mathrm{p}$$

which enables calculation of the coefficient a_p. From the condition $S_\mathrm{p}(x = 0) = 0$ it follows that $C_\mathrm{p} = 0$. The resulting constraint equation

$$\frac{1}{2}x\sqrt{1 + 4a_\mathrm{p}^2x^2} + \frac{1}{4a_\mathrm{p}}\mathrm{arsinh}(2a_\mathrm{p}x) \stackrel{!}{=} S_\mathrm{p,nom} \tag{30}$$

can be solved numerically for the coefficient a_p. The BC at the edge, $y(R) = 0$, finally returns the coefficient

$$c_\mathrm{p} = -a_\mathrm{p}R^2 \tag{31}$$

From this, the reference parabola is completely defined. It is compared to the shape of the catenary with SRP, as obtained from the BVP, and the classical catenary in Fig. 10. The figure shows all three curves with the same slack length of $S = 105\,\mathrm{m}$. Clearly, the classical catenary curve is very similar to the reference parabola, as noted in subsection II.I.

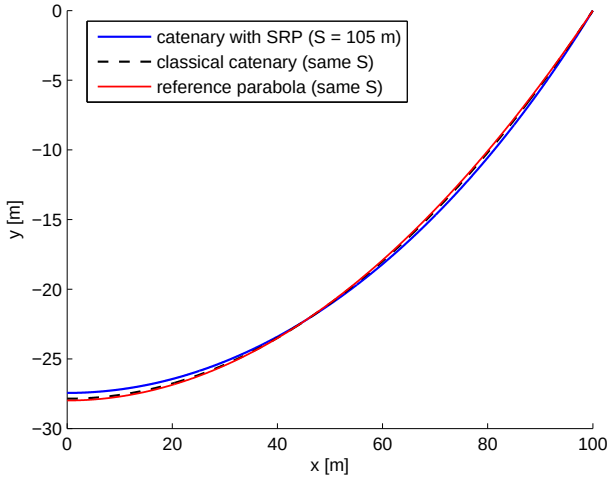

Figure 10: Comparison of inelastic sail film deflection: catenary curve with SRP, obtained from solving the BVP (blue curve), classical catenary (dashed curve) and reference parabola (red curve) with same slack length $S = 105\,\mathrm{m}$

The previously defined parabolic reference deflection curve is now to be created by controlling the reflectivity distribution across the sail surface. For this purpose, an inverse problem is formulated from the equations of section II, which is defined as calculating the necessary reflectivity function $\rho(x)$ to obtain a given sail deflection shape. In doing so, we are replacing the constant reflectivity ρ in in the SRP force equation, Eq. 8, by a generic reflectivity function $\rho(x)$ that varies across the sail surface. Through this, the single ODE of inelastic sail film deflection including SRP (Eq. 19) modifies to

$$y'' = \frac{p_0(1+\rho(x))}{T_{0,\mathrm{p}}}(1+y'^2)^2 \tag{32}$$

Inserting the reference parabola, Eq. 27b and 27c, into the previous equation and solving for the unknown reflectivity function $\rho(x)$, results as

$$\rho(x) = \frac{2a_\mathrm{p}\,T_{0,\mathrm{p}}}{p_0\left(1+(2a_\mathrm{p}x)^2\right)^2} - 1 \tag{33}$$

In order to find an expression for the unknown central tension that matches the parabolic deflection curve $T_{0,\mathrm{p}}$, the additional physical constraint $\rho(R) = 0$ is introduced to Eq. 33. Solving for the central tension gives

$$T_{0,\mathrm{p}} = \frac{p_0\left(1+(2a_\mathrm{p}R)^2\right)^2}{2a_\mathrm{p}} \tag{34}$$

When solving the BVP of Eq. 32 with the previously found $T_{0,\mathrm{p}}$, the resulting sail deflection curve matches the reference parabola, as can be seen in Fig. 11. The required reflectivity distribution across the sail film in the x direction, according to Eq. 21, is shown in Fig. 12.

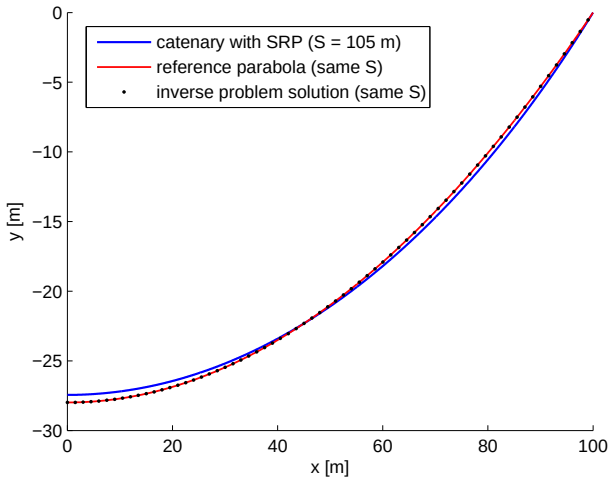

Figure 11: Comparison of catenary curve with SRP, obtained from solving the BVP (blue curve), reference parabola (red curve) and inverse problem solution (dotted curve), creating parabolic sail film deflection (slack length $S = 105\,\mathrm{m}$)

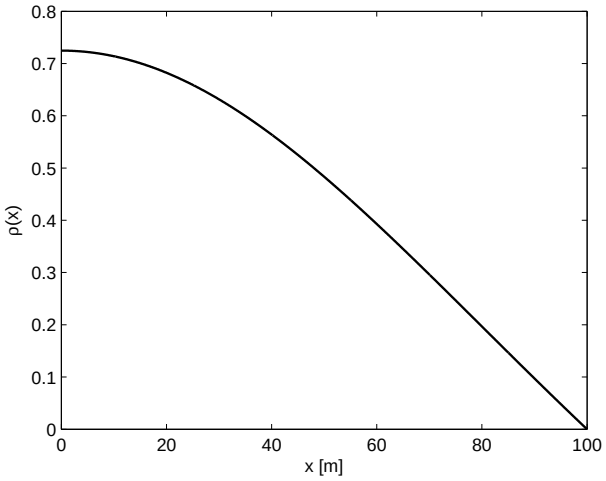

Figure 12: Required reflectivity distribution across sail surface in radial x direction, creating parabolic sail film deflection (slack length $S = 105\,\mathrm{m}$)

A large, highly reflective parabolic surface has many potential applications, such as communication, sensing and power collection. In order to evaluate the usefulness of the shapes that can be generated, the achievable focal lengths will now be identified. A paraboloid concentrates incoming electro-magnetic radiation into a single focal point, depending on the geometrical precision of the surface generated. As already noted above, the focal length can be calculated according to

$$f = \frac{1}{4a_\mathrm{p}} = \frac{R^2}{2|y_0|} \tag{26}$$

when considering the quadratic coefficient $a_\mathrm{p} = -c_\mathrm{p}/R^2 = -y_0/R^2$. Thus, the focal length is a function of surface radius R and its central deflection y_0. The latter depends on the specified slack film length, as seen in Fig. 9. According to this, the focal lengths are calculated for a set of rigid hoop radii $R_i = [1, 5, 10, 25, 50, 100]$, each suspending a sail film of varying slack length $S_{i,\mathrm{nom}} = [101, 102, 103, 104, 105, 106]$ percent R_i. The resulting focal lengths for all deflected sail films are shown in Fig. 13.

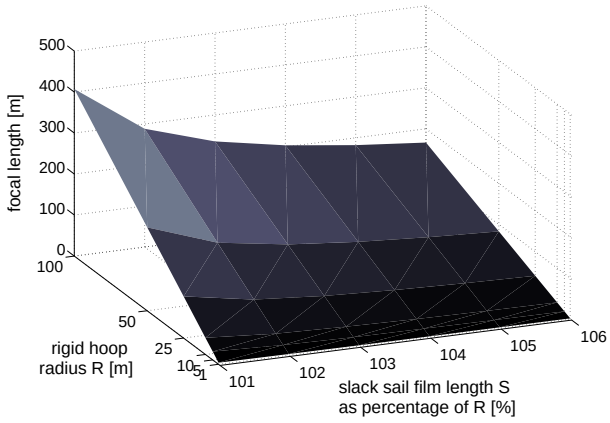

Figure 13: Focal length of deflected parabolic sail surface (of a circular solar sail disk) as a function of sail radius and slack length

V. CONCLUSIONS

A variable reflectivity distribution across the surface of a thin inelastic circular sail film, supported by a rigid hoop structure, has been used to investigate potentially novel mission applications for solar sails. The surface reflectivity can be manipulated when distributing electro-chromic coatings across the sail film or by prefabricating a fixed reflectivity distribution into the surface that allows for a parabolic deflection. This way, the sail could be used as an antenna, telescope or solar concentrator. The sail film has been modelled as a 'cobweb' of radially spanned threads that are not linked in the circumferential direction. The threads are suspended from the rigid hoop structure and intersect at the centre of the circular film. The governing equations of inelastic catenary-type deflection of the surface have been derived. The nominal sail film deflection due to a uniform vertical solar radiation pressure load distribution has been calculated numerically by solving an iterative boundary value problem in Matlab. Using different rigid hoop diameters and slack film lengths, it was shown that the nominal sail deflection is not an ideal paraboloid. Therefore, the deflected sail surface does not concentrate incoming light into a single focal point. However, an analytical expression for the reflectivity function across the surface, necessary to create a true parabolic deflection shape, has been derived. Although limited to sail film attitudes normal to the Sun, this can be used for pre-fabricating a fixed reflectivity distribution into the film surface. This allows for parabolic film deflection at any solar distance, since the obtained deflection shape is independent of the load magnitude. The focal lengths of the resulting parabolic reflectors were calculated for the chosen rigid hoop diameters and slack film lengths. They are typically in the range of a few hundred meters. By positioning a detached platform, formation-flying in the sail film focus, the proposed parabolic sail reflector potentially enables novel mission applications for solar sails.

VI. ACKNOWLEDGEMENT

This work was funded by the European Research Council Advanced Investigator Grant - 227571: VISIONSPACE: Orbital Dynamics at Extremes of Spacecraft Length-Scale.

REFERENCES

[1] C. R. McInnes. *Solar Sailing: Technology, Dynamics and Mission Applications*. Springer-Praxis Series in Space Science and Technology, 1999.

[2] C. R. McInnes. Delivering fast and capable missions to the outer solar system. *Advances in Space Research*, 34(1):184–191, 2004.

[3] H. Demiryont and D. Moorehead. Electrochromic emissivity modulator for spacecraft thermal management. *Solar Energy Materials and Solar Cells*, 93(12):2075–2078, 2009.

[4] L.F. Troyano. *Bridge Engineering: A Global Perspective*. Thomas Telford, 2003.

[5] Math24.net. http://www.math24.net/equation-of-catenary.html, 2013. [Online; accessed 05 July 2013].

[6] E.H. Lockwood. *Book of Curves*. Cambridge University Press, 1961.

[7] L.F. Shampine, I. Gladwell, and S. Thompson. *Solving ODEs with MATLAB*. Cambridge University Press, 2003.